

Article

Modeling Mixed Traffic Flow with Connected Autonomous Vehicles and Human-Driven Vehicles in Off-Ramp Diverging Areas

Xiangquan Chen ¹, Zhizhou Wu ¹ and Yunyi Liang ^{2,*}

¹ Key Laboratory of Road and Traffic Engineering of the Ministry of Education, Tongji University, Shanghai 201804, China

² School of Transportation Engineering, Central South University, Changsha 410083, China

* Correspondence: 22022049@csu.edu.cn; Tel.: +86-136-6176-4613

Abstract: This paper focuses on modeling mixed traffic flow that comprises human-driven vehicles (HV), adaptive cruise control (ACC) vehicles, and cooperative adaptive cruise control (CACC) vehicles in the off-ramp diverging area. The car-following behaviors of HVs, ACC vehicles, and CACC vehicles are modeled using an intelligent driver model (IDM), ACC car-following model, and CACC car-following model, respectively. The lane-changing behaviors of different types of vehicles in off-ramp diverging areas are modeled using the anticipatory lane change (ALC) model and the mandatory lane change (MLC) model. These models are important for describing the interaction among different types of vehicles in mixed traffic. The safety and efficiency of mixed traffic flow are analyzed by integrating the developed car-following models and lane-changing models in numerical simulation. A one-way, two-lane scenario is established for the simulation. The results reveal that when the proportion of CACC vehicles is about 0.6, the safety and general operating efficiency of mixed traffic flow in the off-ramp area deteriorate significantly. Increasing the conservative MLC zone length can improve the average speed of traffic flow. Guiding drivers in changing lanes is one way to improve the efficiency of traffic flow.

Keywords: mixed traffic flow; cooperative adaptive cruise control; car-following; lane-changing; off-ramp diverging areas



Citation: Chen, X.; Wu, Z.; Liang, Y. Modeling Mixed Traffic Flow with Connected Autonomous Vehicles and Human-Driven Vehicles in Off-Ramp Diverging Areas. *Sustainability* **2023**, *15*, 5651. <https://doi.org/10.3390/su15075651>

Academic Editor: Luca D'Acerno

Received: 31 January 2023

Revised: 15 March 2023

Accepted: 21 March 2023

Published: 23 March 2023



Copyright: © 2023 by the authors. Licensee MDPI, Basel, Switzerland. This article is an open access article distributed under the terms and conditions of the Creative Commons Attribution (CC BY) license (<https://creativecommons.org/licenses/by/4.0/>).

1. Introduction

In recent years, a series of advanced sensors, controllers, and solutions have facilitated the birth of connected autonomous vehicles. Connected and automated driving technology has great potential in terms of traffic safety [1,2], road capacity [3,4], fuel consumption [5–7], driving experience [8], etc.

The off-ramp is a bottleneck section that affects the mainline traffic of the freeway and is a zone that is prone to accidents and congestion. Alleviating the traffic congestion in the bottleneck section of the off-ramp can effectively improve the general operating efficiency and driving safety of the transportation system. In research related to the modeling of off-ramp traffic flow, Dong et al. [9] introduced a risk factor into the discretionary lane-change model and designed a five-step mandatory lane-change decision-making model for connected autonomous vehicles when exiting the off-ramp. Zhang et al. [10] analyzed the influence of lane-changing strategy on three traffic parameters from the perspective of combining traffic control and variable speed limits.

Cooperative adaptive cruise control (CACC) and adaptive cruise control (ACC) are widely used in vehicles with high driving automation levels [11,12] to control the longitudinal motion of vehicles. CACC vehicles obtain the speed, position, and other driving information that is actively transmitted by surrounding vehicles through the vehicle-to-vehicle communication system. ACC vehicles observe the information from surrounding

vehicles through onboard units, radar, and other detection equipment. Research on traffic flow utilizes microscopic modeling and operation characteristics and is the primary focus of the traffic engineering field. In research applying the car-following model, the full-speed difference model [13] and the intelligent driver model [14] are widely used to simulate the car-following behavior of manually operated vehicles. The CACC model and ACC model proposed by the PATH laboratory of the University of California, Berkeley, USA from real vehicle tests are often used as the basic model to describe the lane-changing behavior of connected autonomous vehicles [15–17]. To develop this approach, Hidas [18] divided lane-changing behavior into three types: random lane change, anticipatory lane change (ALC), and mandatory lane change (MLC). In the case of random lane change, Yang [19] analyzed the impact of its implementation on the following and preceding vehicles. The lane-changing model thus constructed can better reflect the impact on traffic flow of the interference process between vehicles. Zheng et al. [20] divided the transition induced by lane-changing into an anticipation component and a relaxation component. Compared with random lane changing, mandatory lane changing mostly exists near intersections and on-ramp and off-ramp systems [21], which very easily cause bottlenecks in the traffic system. Presently, the research suggests that the closer the vehicle is to the exit point, the higher the probability of the driver implementing a mandatory lane change. However, the existing methods do not take into account the differences between CACC vehicles and HVs in terms of data acquisition, information processing, and decision-making actions and lack a description of the horizontal interaction between the two types of vehicles.

There is little research into the off-ramp lane change model of connected autonomous vehicles in the existing literature. On the one hand, the freeway has heavy traffic flow and fast speeds. The off-ramp diverging area is the area where the mainline vehicles and the off-ramp vehicles are intertwined. There are right-of-way conflicts and the traffic organization is relatively chaotic, which makes traffic accidents more likely. The complex road environment determines the complexity of the research object. On the other hand, most of the existing lane change models are only applicable to human-driven vehicles (HV), not to mixed traffic flow, and the lane change model of the off-ramp diverging area is more complex than that of the basic road section. These issues lead to insufficient research into the modeling of mixed traffic flow in the off-ramp area.

The main objective of this study is to model the car-following and lane-change behaviors of CACC vehicles, ACC vehicles, and HVs in off-ramp areas and their impacts on traffic safety and efficiency. The remainder of this paper is structured as follows: Section 2 introduces related works in the literature, while Sections 3 and 4 present the car-following model and the lane-changing model, respectively. In Section 5, the simulation scheme and analysis index are described in detail. Traffic safety and the efficiency of mixed traffic flow are analyzed via simulation in Section 6. Our concluding remarks and a discussion of future work are given in Section 7.

2. Related Works

Research on traffic flow via microscopic modeling and operation characteristics is the focus of traffic engineering. The car-following model is the basis for explaining the evolution of traffic flow at the micro-level. In the traditional car-following model, the stimulus–response model is represented by the GM model [22] and the Newell model [23]. A car-following model based on cognitive psychology is represented by the physiological–psychological car-following model established by Wiedemann, which has become the core model of many famous micro-simulation software programs, such as VISSIM. Traffic engineering models can effectively reflect the impact of the subjective judgment and operation of the driver in terms of vehicle-following. It focuses on accurately fitting the measured driving data at the micro-level. Models developed on the basis of cellular automata theory, such as Rule 184 and its extended NaSch model, can better explain the essence of traffic element dispersion [24]. The time, space, and vehicle speed are all discretized by integers. The discrete and finite cells can accurately simulate the evolution law of a complex system

in the two dimensions of time and space. With the development of connected autonomous vehicles, a new generation of connected autonomous assisted driving systems based on constant-speed cruise control systems, such as ACC and CACC, has emerged [25,26]. The PATH laboratory of the University of California, Berkeley, USA, conducted long-term research on the ACC/CACC system and calibrated the parameters of the ACC/CACC car-following model through real vehicle testing. Therefore, the traffic flow theoretical research based on such models can objectively describe the impact of ACC/CACC vehicles on the traffic flow characteristics [15]. The intelligent driver model (IDM) constructed by Treiber et al. [14] describes typical car-following behavior, taking into account the expected speed, car-following distance, and the asymmetric behavior of the acceleration and deceleration processes caused by the habits of the driver or vehicle acceleration/deceleration performance differences. IDM reflects the accurate perception and operation of the connected autonomous auxiliary equipment. The optimized improved model has become a typical representative of the ACC/CACC vehicle car-following behavior model and has been widely used.

As the most basic driving behavior, lane changing is an important part of traffic flow theory. The different motivations for lane changes can be divided into anticipatory lane changes and mandatory lane changes. From the perspective of lane-change behavior modeling, most of the models are based on the modeling research proposed by Ahmed et al. [27], in which the lane-change process is divided into four discrete processes: motivation generation, lane selection, gap selection, and lane change execution. There are few studies on the comprehensive strategy modeling of mandatory lane change and anticipatory lane change in the off-ramp area of urban roads or expressways. In their study [28], Zhang et al. used the Shanghai natural driving research (SH-NDS) data to study the lane-change characteristics of the off-ramp area of the expressway under different traffic conditions. A discrete selection framework is adopted in lane-change decisions, and utility functions that are weighted by different parameters are constructed. The concept of utility is used to measure the satisfaction of changing to the target lane under specific traffic conditions and driving routes. The research results show that the lane-change behavior of exiting vehicles is the result of a balance between path planning (mandatory incentive) and the expectation of improving driving conditions (discretionary incentive). To some extent, it reveals the mechanism of lane-change behavior in the off-ramp area, the factors that affect lane-change behavior under different traffic conditions, and the preference of the driver. The decision model used in this study is an instant decision model based on the current traffic scenario. In one previous study [9], the modified comfortable driving car-following rule and the PATH car-following model are used to simulate the longitudinal movement of vehicles. Based on the characteristics of human-driven vehicles and connected autonomous vehicles, parameters such as the vehicle perception range, lane-change control area, and lane-change risk factor are introduced to establish anticipatory lane-change and mandatory lane-change models that control the lateral movement of vehicles. Through numerical simulation, the influence of the generation probability of mainline vehicles, the proportion of off-ramp vehicles, the CACC vehicle penetration rate, the vehicle perception range, the length of the lane-change area, and the risk degree of lane changes on the traffic flow is explored. The research shows that the larger the vehicle perception range, the longer the lane-change area length, and the greater the risk of lane change; it is possible to improve the operation efficiency of the mixed traffic system, which has a positive effect on delaying the generation of congestion and accelerating the dissipation of congestion.

Mandatory lane changes in the off-ramp area often seriously affect traffic capacity and stability, so it is necessary to alleviate traffic congestion. In their study of suggestions for alleviating traffic congestion, Nafi et al. [29] proposed a predictive road traffic management system (PRTMS) based on a vehicular ad hoc network (VANET) architecture. The proposed PRTMS uses a new communication scheme to estimate the future traffic intensity at different intersections based on the improved linear prediction algorithm. The simulation is conducted using the comprehensive OPNET model. The scheme has a significant performance

improvement in the total travel time and waiting time of vehicles. Zambrano-Martinez et al. [30] proposed a centralized traffic manager that can deal with all the traffic in the city and balance the traffic flow by considering current and future traffic congestion conditions. This simulation study was performed using real traffic congestion data from Valencia, Spain. The experimental results show that the proposed traffic prediction equation can achieve a significant improvement in the average travel speed and travel time.

In general, the current research results on traffic flow characteristics focus on describing a traffic environment composed of a single driver-type scenario, such as pure manual driving traffic flow, pure ACC/CACC traffic flow, or pure connected autonomous vehicle traffic flow; there are few studies on the comprehensive strategy modeling of mandatory lane changes and free lane changes in the off-ramp areas of freeways. Unlike previous studies based on the driving characteristics of vehicles in the bottleneck section of the off-ramp, our research has established a mixed car-following rule and lane change rule for a variety of driver types. On this basis, we have analyzed the characteristics of heterogeneous traffic flow and explored traffic flow operation in the bottleneck section under the influence of different factors.

3. Car-Following Model for Mixed Traffic Flow

The off-ramp area of the freeway consists of the mainline, the off-ramp, and the connecting area. Freeways are generally multi-laned in the same direction. When vehicles drive in the left or right lane, the target lane is only generated in the current lane and the middle lane. When the vehicle is located in the middle lane, there are three options for changing lanes. Although the number of lanes available for vehicles in the above two cases is different, for vehicles changing lanes, there are only two options: continue to drive in the current lane or change lanes to the adjacent lanes. Therefore, for convenience, the road in the freeway scenario is simplified into two lanes running in the same direction, as shown in Figure 1. Vehicles in the mainline segment perform both following and lane-changing behaviors. Vehicles with the intention to exit the freeway gradually change lanes to the right until they leave the mainline segment.

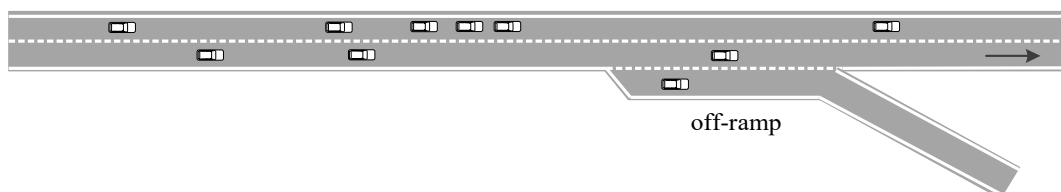


Figure 1. Mixed traffic flow in an off-ramp diverging area.

3.1. Car-Following Model for HVs

Research into car-following models of human-driven vehicles is relatively mature, and most of the studies have been calibrated using measured traffic data. Since the object of this study is high-grade roads, the IDM model [14,31] has been selected to describe the car-following characteristics of human-driven vehicles. The formula for this is shown in Equations (1) and (2), while the definitions of symbols appearing in the IDM model are shown in Table 1.

$$\dot{v}_n(t) = a \left[1 - \left(\frac{v_n(t)}{v_0} \right)^4 - \left(\frac{s^*(v_n(t), \Delta v_n(t))}{h_n - l} \right)^2 \right] \quad (1)$$

$$s^*(v_n(t), \Delta v_n(t)) = s_0 + v_n(t) \cdot T - \frac{v_n(t) \cdot \Delta v_n(t)}{2\sqrt{ab}} \quad (2)$$

Table 1. List of symbols in the IDM model.

Parameter	Definition
a	starting acceleration (m/s ²)
b	comfortable deceleration value (m/s ²)
$v_n(t)$	vehicle speed (m/s)
v_0	free flow speed (m/s)
$s^*(\cdot)$	desired spacing (m)
s_0	safe stopping distance (m)
T	safety headway (m)
$\Delta v_n(t)$	speed difference between the subject vehicle and preceding vehicle (m/s)
h_n	distance between the subject vehicle and preceding vehicle (m)
l	vehicle length (m)

The model parameters have previously been calibrated in [32]. The calibration values of the IDM model parameters are shown in Table 2.

Table 2. IDM model parameter calibration values.

Parameter	Value
a (m/s ²)	1
b (m/s ²)	2
v_0 (km/h)	120
s_0 (m)	2
T (s)	1.5
l (m)	5

3.2. Car-Following Model for ACC Vehicles

We adopted the model proposed and verified by the PATH Laboratory of the University of California, Berkeley as the car-following model [15]. This adopts the constant headway strategy and has been verified by real vehicle experiments, which can better reflect the car-following characteristics of ACC vehicles. The ACC car-following model is shown in Equation (3):

$$\dot{v}_n(t) = k_1[x_{n-1}(t) - x_n(t) - t_a v_n(t) - l - s_0] + k_2[v_{n-1}(t) - v_n(t)] \quad (3)$$

where $\dot{v}_n(t)$ is the acceleration of vehicle n at time t , and $x_n(t)$ and $x_{n-1}(t)$ are the displacements of vehicle n and $n - 1$ at time t . $v_n(t)$ and $v_{n-1}(t)$ are the speeds of vehicle n and $n - 1$ at time t . l is the vehicle length. s_0 is the safe stopping distance. t_a is the expected time headway of ACC. k_1 and k_2 are the control coefficients. According to a previously reported vehicle experiment [17], their values are 0.23 and 0.07, respectively.

3.3. Car-Following Model for CACC Vehicles

For CACC vehicles, the CACC model proposed by the PATH laboratory is used to describe their car-following behavior. The vehicle speed is continuously adjusted by the error term of the actual and expected spacing. The car-following model of AV is given by Equations (4) and (5) [16]:

$$v_n(t) = v_p + k_p e_n(t) + k_d \dot{e}_n(t) \quad (4)$$

$$e_n(t) = \Delta x_n(t) - s_0 - l - t_c v_n(t) \quad (5)$$

where v_p is the speed of the last control period. $e_n(t)$ is the error between the actual vehicle spacing and the expected vehicle spacing. $\dot{e}_n(t)$ is the derivative of e and t_c is the expected time headway of CACC. k_p and k_d are the control coefficients. According to the vehicle experiment in [17], their values are 0.45 and 0.25, respectively.

The velocity in the above formula is derived using Equation (6):

$$\dot{v}_n(t) = \frac{k_p(\Delta x - s_0 - l) - k_p t_c v_n(t) + k_d \Delta v_n(t)}{k_d t_c + t_1} \quad (6)$$

where the values of each parameter are as follows: $t_c = 0.6$ s, $k_p = 0.45$, $k_d = 0.25$, and $t_1 = 0.01$ s [15,17,33].

4. Lane-Changing Model for Mixed Traffic Flow

We established the lane-change decision flow chart (Figure 2) based on the lane-change process proposed by Hidas [18].

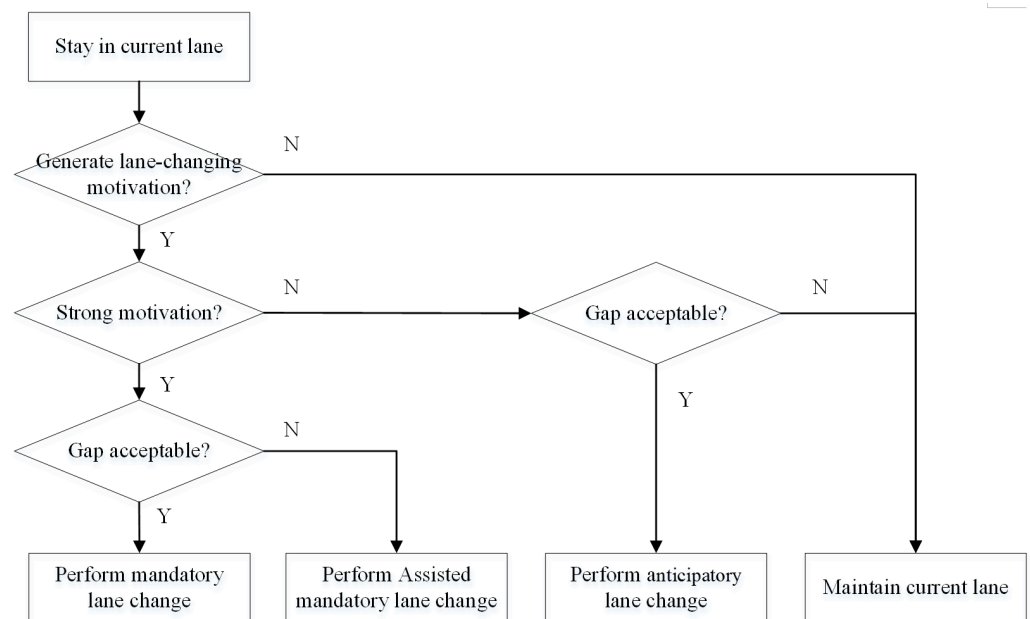


Figure 2. Flow chart of lane change decisions.

Depending on the different lane-change motivations, the lane-changing mode is divided into two types: ALC and MLC. In the case of MLCs in the diverging area, the decision-making behavior of the driver can be divided into two stages: the conservative stage and the aggressive stage. The main purpose of an ALC is to obtain a speed advantage or better driving conditions. The main purpose of an MLC is to reach the destination.

The zone division for exiting vehicles is shown in Figure 3. All vehicles implement a stable car-following model in the upstream area of zone 1. Vehicles in zone 1 implement an ALC behavior. If the lane-change motivation is greater than the expected lane-change threshold, finding the gap between adjacent right lanes and implementing a lane-change maneuver occurs if the gap is acceptable. The vehicle will perform an MLC if the lane change has not been completed in zone 1. The time when the MLC produces motivation also has a certain impact on driving efficiency. Vehicles in zone 2 perform conservative MLCs. Vehicles changing lanes at this stage will not affect the vehicles following them. Generally, the vehicle at the front turns to the second stage of MLC in zone 3, when the distance between it and the exit is equal to the shortest distance required for changing lanes. However, in practice, 96% [34] of diverging vehicles begin to change lanes in the middle of the deceleration lane, but only for the two-lane diversion area. For multiple lanes, this psychological feature is most obvious in the left lane. The starting position of MLC (the distance from the exit) dynamically changes within a certain range, due to the perception of distance and the intensity of demand of the driver.

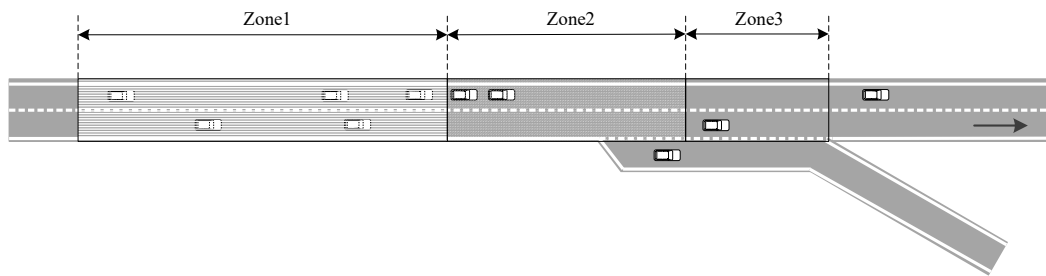


Figure 3. Zone division for exiting vehicles.

As shown in Figure 2, lane-change behavior can be divided into three stages: the generation of lane-change motivation, safety judgments, and the implementation of lane-changing behavior. The following sections will quantify the lane-change behavior process into a specific formula expression, to more accurately simulate the lane changes of automatic driving vehicles on the off-ramp.

4.1. Anticipatory Lane Change

When the current speed of the vehicle is less than the desired speed, driver dissatisfaction comes from the gap between the current speed and the desired speed. The cumulative degree model of speed dissatisfaction is used to measure driver dissatisfaction. The speed dissatisfaction accumulation describes the cumulative amount of the difference between the desired speed and the actual speed over time. The larger the gap between the desired speed and the current speed, the greater the dissatisfaction value. This means that the driver is more psychologically dissatisfied with the driving speed. This model is expressed by Equation (7):

$$V_n(t) = V_n(t-1) + \frac{v_{des} - v_n(t)}{v_{des}} \Delta t \quad (7)$$

where $V_n(t)$ is the cumulative degree of speed dissatisfaction of the vehicle n at time t . Δt is the sample time. When $V_n(t)$ is greater than the set threshold, the vehicle will be triggered to change lanes.

It is only when the speed dissatisfaction accumulation exceeds the set dissatisfaction accumulation threshold, V_{thr} (Equation (8)) that the vehicle has the intention of changing lanes. In the case of HV, when the vehicle speed dissatisfaction accumulation exceeds the dissatisfaction accumulation threshold, the vehicle generates a lane-changing motivation with a probability of P_{ALC} . The probability value is generated by a random function. For ACC/CACC vehicles, the control system will change lanes when the lane change conditions are met, so the lane change probability is 1.

$$v_n(t) < V_{thr} \quad (8)$$

It is necessary to judge whether the vehicle can complete the lane-change maneuver safely and without collision after the intention of a lane change is generated. The driver evaluates the gap in the target lane to judge whether the lane-change maneuver can be performed. When the safety distance conditions in Equations (9)–(11) are satisfied, the vehicle performs the desired lane change:

$$d_{p,n}(t) > d_n(t) \quad (9)$$

$$d_{p,n}(t) > d_{p,safe} \quad (10)$$

$$d_{f,n}(t) > d_{f,safe} \quad (11)$$

where $d_{p,n}(t)$ is the distance between vehicle n and the preceding vehicle on the adjacent lane at time t . $d_{f,n}(t)$ is the distance between vehicle n and the following vehicle on the adjacent lane at time t . $d_n(t)$ is the distance between vehicle n and the preceding vehicle

in the current lane at time t . d_{safe} is the safe distance, that is, the distance between the following vehicle and the preceding vehicle after emergency braking. d_{safe} is calculated using Equation (12):

$$d_{safe} = (v_n(t)t_{reaction} + \frac{v_{n-1}^2(t)}{2a_n}) - (\frac{v_{n-1}^2(t)}{2a_{n-1}} - l) \quad (12)$$

where a_n is the maximum deceleration of the vehicle n . l is the vehicle length. $t_{reaction}$ is the reaction time. In this study, the reaction time is taken to be 1.5 s for human-driven vehicles, 0.6 s for CACC vehicles, and 1.0 s for ACC vehicles.

4.2. Mandatory Lane Change

For a conservative MLC, the generation of motivation only considers the distance from the vehicle to the end of the off-ramp. The probability of aggressive MLC motivation is 1. The generation of MLC motivation is shown in Equations (13) and (14):

$$P_{MLC,c} = 1 - \left(\frac{d - E_3}{E_2 - E_3} \right) (E_3 < d \leq E_2) \quad (13)$$

$$P_{MLC,a} = 1 (d \leq E_3) \quad (14)$$

where E_2 and E_3 are the length from the starting point of zone 2 to the end of the off-ramp and the length from the starting point of zone 3 to the end of the off-ramp, respectively.

After the MLC motivation is generated, the vehicle will assess whether the safety condition for a lane change is satisfied (Equations (10) and (11)). If it is, the vehicle will perform the lane-changing maneuver. When the lane-changing condition in the adjacent lanes is still not satisfied, the subject vehicle moves the following target from the preceding vehicle of this lane change to the preceding vehicle of the target lane. At the same time, the vehicle following in the target lane changes its target to the subject vehicle to assist it in completing a lane-changing maneuver. CACC vehicles are more active than HVs in assisting other vehicles in changing lanes. They have a stronger willingness to adopt cooperative lane changing, that is, actively slowing down to create a gap for an MLC maneuver.

The car-following strategy is calculated according to the different car-following models selected by the preceding vehicle as the HV, ACC vehicle, or CACC vehicle. When changing lanes, the maneuver will be conducted when the safety conditions are satisfied.

5. Simulation Scheme

For our experimentation, we used the simulation software SUMO-1.8.0 to construct simulation scenarios. SUMO (simulation of urban mobility) is a highly portable micro-traffic simulation package developed and open-sourced by the Institute of Transportation Systems of the German Aerospace Center [31]. SUMO offers the characteristics of open-source software, an intuitive visual interface, good platform adaptability, and excellent flexibility. SUMO is gradually becoming the preference of many researchers and has been chosen here as the simulation software for studying automatic driving.

SUMO provides an external connection interface called the traffic control interface; this experiment used Python-3.6.1 for secondary development on its framework. In SUMO, after establishing the road network model, it is necessary to edit the traffic flow file to establish a completely heterogeneous traffic flow simulation scene. The readable traffic flow files in SUMO include the design traffic parameters, vehicle parameters, traffic flow models, and other information. According to the following values of the traffic vehicle and route parameters, utilizing the open-source nature of SUMO simulation software, a program was written using the Python platform to call the car-following model and lane-changing model of connected autonomous vehicles and human-driven vehicles, respectively, to control each vehicle individually.

The simulation scenario was established as shown in Figure 3. The length of the mainline was set at 3 km. The initial lengths of zone 1, zone 2, and zone 3 were set to 1000 m, 500 m, and 150 m, respectively. The maximum speed of the two lanes of the mainline was limited to 100 km/h and 80 km/h from the inside out. The initial traffic volume of the main freeway was set at 2000 vehicles per hour, and the proportion of vehicles leaving the freeway was 0.1. The simulation lasted 3600 s, and each simulation step was 0.1 s.

We conducted three simulation experiments in parallel under the same conditions and took the average value as the result. The simulation model parameters are shown in Table 3.

Table 3. The simulation model's parameters.

Parameter	Value		
	HVs	CACC Vehicles	ACC Vehicles
maximal speed (m/s ²)	33.3	33.3	33.3
maximum acceleration (m/s ²)	2.5	3	3
minimum acceleration (m/s ²)	4.0	4.5	4.5
reaction time (s)	1.5	0.6	1.0

Traffic safety and traffic efficiency were selected as the analysis indicators of the dynamic characteristics of mixed driving traffic flow.

Time to collision (TTC) is the time taken for the subject vehicle and preceding vehicle to collide when maintaining the current speed difference. TTC is widely used in the field of traffic flow safety evaluation, including a traffic flow environment that is mixed with AV. The TTC of a vehicle is calculated by Equation (15) if the speed of the vehicle $n - 1$ is lower than the speed of n . Otherwise, TTC equals infinity.

$$TTC_n(t) = \frac{\Delta x_n(t) - l}{\Delta v_n(t)}, \forall v_n(t) > v_{n-1}(t) \quad (15)$$

The collision risk of each vehicle is different, so TET (time of exposed TTC) is often used for safety evaluation. TET is the total time exposed to dangerous conditions. It is an expanded evaluation index based on TTC and can be described by Equation (16):

$$TET = \sum_{n=1}^N \sum_{t=1}^M \delta_n(t) \Delta t \quad (16)$$

where N is the total number of vehicles in the traffic flow. M is the total simulation time. When the TTC of the vehicle n is greater than 0 and less than or equal to the collision time threshold, TTC^* , $\delta_n(t)$ is equal to 1. Otherwise, $\delta_n(t)$ is equal to 0. The collision time threshold indicates the acceptable degree of rear-end collision risk. The greater the value of TET, the higher the collision risk. TTC^* is usually taken as 1~3 s. In this research, we take 3 s as the threshold.

6. Discussion

When the initial traffic volume and the proportion of off-ramp vehicles are unchanged, this makes the CACC market penetration change from 0.1 to 1. We counted the corresponding TET distribution under the low off-ramp vehicle ratio and high off-ramp vehicle ratio, where $\alpha = 0.1$ and $\alpha = 0.5$. As shown in Figure 4, the TET value first increased and then decreased. When the CACC market penetration was 0.5, TET reached its peak and then began to decline. This shows that when the CACC market penetration is low, the safety problem of mixed traffic flow in the off-ramp area is more serious than the homogeneous traffic flow formed by human-driven vehicles. When the penetration is close to 100%, the value of TET decreases sharply.

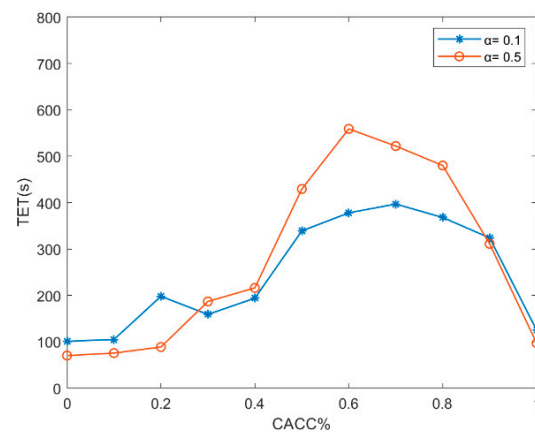


Figure 4. The TET curve under different CACC market penetration and off-ramp vehicle ratios.

The reason for this is that there are differences in the car-following and lane-changing behaviors of different types of vehicles. When fewer CACC vehicles are distributed in the traffic flow, the degradation phenomenon is serious. In this scenario, either the preceding vehicles of CACC vehicles are human-driven vehicles, or the following vehicles of human-driven vehicles are CACC vehicles. The behavior of vehicles in the off-ramp area is complex, and this phenomenon increases the insecurity of traffic flow. However, when the CACC market penetration increases to a certain extent, the mixing rate of ACC and HV decreases, and CACC vehicles become the main component of the traffic flow. CACC vehicles can better perceive the states of the vehicles in front through the sensing system, and the following time headway and reaction time are short, so they can maintain a relatively stable distance and speed with the preceding vehicle, avoiding dangerous situations. Therefore, the TET value decreases significantly when CACC market penetration increases.

Figure 4 also compares the TET values under different off-ramp vehicle ratio conditions. The results show that TET in a high CACC market-penetration range changes sharply with a high off-ramp vehicle ratio. Compared with the simulation results of a low off-ramp vehicle ratio, when the permeability is greater than 0.5, the TET increases rapidly, indicating that vehicles spend more time exposed to danger. When off-ramp vehicles increase, the number of implemented lane-changing maneuvers increases. In this scenario, fewer HVs are distributed in the CACC flow and cause greater interference. At the same time, the headway between CACC vehicles is much smaller than with HV. Frequent lane-changing behavior leads to an increase in the total time of cumulative exposure to dangers. When CACC penetration is at 100%, the traffic flow is completely stable, and TET has fallen to a very low level.

The change in average speed with CACC market penetration also goes through a process of first decreasing and then increasing, as shown in Figure 5. When CACC penetration is very small or very large, the traffic flow can be stabilized at a higher average speed. When CACC penetration changes from 0.2 to 0.8, the heterogeneity of traffic flow makes the average speed low, and it reaches its lowest level when the penetration is about 0.4. When the proportion of CACC is higher than 0.8, the average speed of traffic flow has been significantly improved. The characteristics of short headway and the fast response of CACC vehicles have been transformed into a higher average running speed.

Figure 5 also compares the average speed under different off-ramp vehicle ratios. The simulation results show that the average speed is not very sensitive to the off-ramp vehicle ratio, while the changing trend of the average speed is basically the same. At low and high CACC penetration values, the average speed of the vehicles shows little difference. In the range of 0.2 to 0.8, the average speed difference between the two ratios is about 1 m/s^2 . Because the length of the lane-change area is fixed, an increase in the total number of lane changes must be accompanied by an increase in the number of MLC maneuvers. The forced insertion of vehicles will slow down the following vehicles and reduce general

traffic efficiency. However, this result shows that under this traffic density, the off-ramp vehicle ratio will not have a dramatic impact on traffic efficiency.

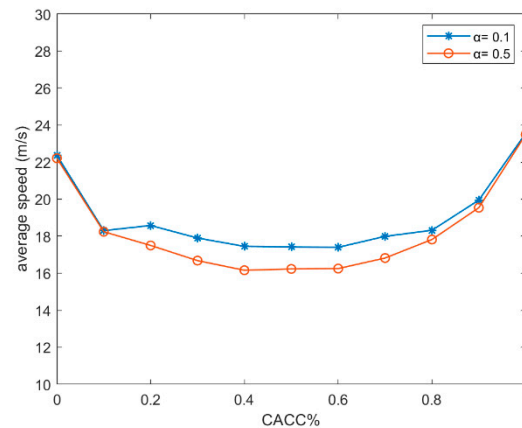


Figure 5. The average speed curve under different CACC market penetration and off-ramp vehicle ratios.

Berrazouane et al. [35] leveraged calibrated SUMO traffic simulation models to analyze the effects of the penetration rate of automated vehicles on the safety and efficiency of mixed traffic flow. The conclusion drawn in their study is that when the permeability changes from 0% to 100%, the operation of traffic flow will gradually deteriorate along with the increase in the penetration of connected autonomous vehicles. This is different from the results obtained in the current study because of the different modeling control logic. Their research did not collect the flow data for the off-ramp, so the results could not accurately reflect the traffic flow operation near the ramp. The research in this paper redevelops the lane-change model according to the operation of off-ramp traffic flow so it can better reflect the behavior of different types of vehicles in a certain area of the off-ramp.

Lane-change maneuvers in the off-ramp diversion area are the main cause of traffic disturbance. The timing of MLC motivation also has an impact on traffic flow characteristics. Therefore, we also tested the traffic efficiency of the conservative MLC area when the length of zone 2 changed. Figure 6 shows the simulation results of the average speed of traffic flow as it changes with the CACC penetration rate and the off-ramp ratio. The abscissa represents the off-ramp ratio, the ordinate represents the CACC penetration rate, and the color bar changes gradually from blue to red, indicating that the average speed of traffic flow gradually increases from low to high. First of all, on the whole, the red color is concentrated in places where the CACC penetration rate is particularly low or high, indicating that the traffic flow has a high and stable average speed level in this scenario. When the length of zone 2 increases from 250 m to 750 m, the red color deepens, and the range of the red area extends. Especially in areas with a CACC% penetration rate of 0.3–0.7 and a low off-ramp vehicle ratio, the average speed level has been significantly improved. However, in the case of a high off-ramp vehicle ratio, increasing the length of the Zone 2 area does not improve traffic flow operation. This phenomenon can be observed in the right-hand area of each sub-graph, where the average speed has always been maintained at a low level. The closer the distance from the start of the MLC to the ramp, the higher the proportion of times that vehicles implement MLC maneuvers when approaching the off-ramp, and the greater the negative impact on the general traffic-flow operation. When the location of the MLC motivation is set to be further away from the off-ramp, the vehicles can change lanes ahead of time and avoid changing lanes near the off-ramp, which can effectively relieve the pressure of centralized lane changes and improve the overall operational efficiency of traffic flow. However, when the demand for the off-ramp increases, a large number of vehicles need to change lanes within a certain length of the area. This situation has an impact on traffic operation beyond the range that can be adjusted by early warnings of

lane change and may even cause congestion. In addition, as seen in Figure 6c,d, there is no obvious change in the color of the picture; that is, the length of the forced lane change area has increased from 750 m to 1000 m, which makes no contribution to the improvement of the average speed of traffic flow. This shows that for a certain proportion of off-ramp vehicles, a sufficiently long mandatory lane-change reminder area is sufficient to allow vehicles to change lanes in advance, and it is meaningless to extend the length at this time.

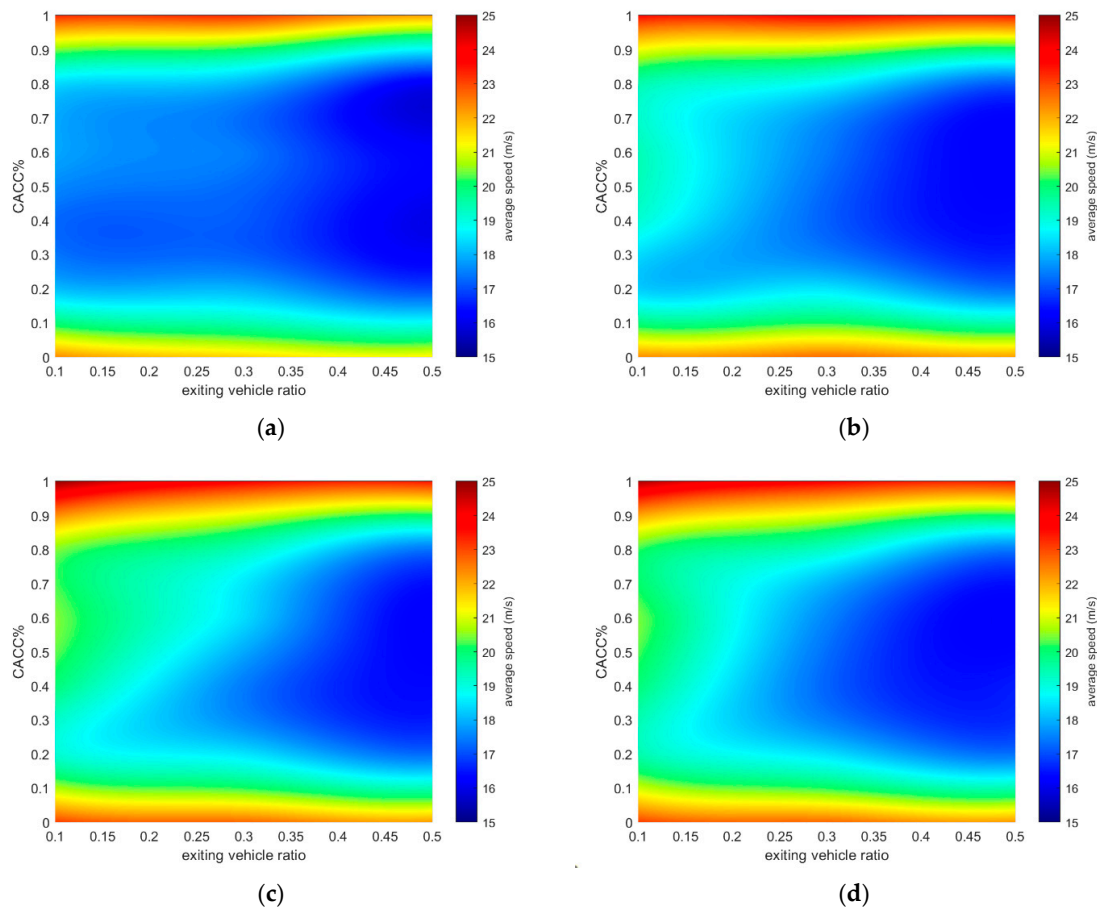


Figure 6. Heat map of the average speed vs. CACC market penetration and off-ramp vehicle ratios under different zone 2 lengths: (a) 250 m; (b) 500 m; (c) 750 m; (d) 1000 m.

7. Conclusions and Future Work

Due to the limitations of the traditional microscopic car-following model theory, the research on traffic flow always utilizes the same car-following rule and lane change rule. However, mixed traffic flow is, in fact, composed of different drivers who follow different driving rules. Compared with human-driven vehicles, connected autonomous vehicles demonstrate better performance in terms of information perception and decision-making judgments. In this paper, a car-following and lane-changing model suitable for describing different types of vehicles in the off-ramp area is established, and simulation experiments are accomplished. The authors used the IDM model and the PATH vehicle experimental car-following model to simulate the longitudinal movement of vehicles and establish the ALC and MLC models, based on the operating characteristics of off-ramp vehicles. Through simulation experiments, we explored the effects of different CACC vehicle penetration rates, off-ramp vehicle ratios, and conservative MLC zone lengths on traffic flow, and the following conclusions were drawn:

- (1) In the off-ramp area of the freeway, CACC vehicle penetration has a significant impact on the safety of mixed traffic flow. When CACC penetration is low, degradation occurs, which increases system instability, including a decline in safety and general

operating efficiency. The traffic flow operation improved significantly when CACC vehicle penetration was close to 1.

- (2) Increasing the conservative MLC zone length can improve the average speed of traffic flow, to a certain extent. When the length of the area is 750 m, the operation of traffic flow shows the best performance. However, the improvement of indicators is not obvious in too-long regions. This has a certain reference value in terms of regulating the congestion of the road traffic system; guiding drivers to change lanes is one way to improve the efficiency of traffic flow.

Our research also has certain limitations. The model established in this paper and the setting of conditions in the simulation experiment are within a reasonable range, but there is a certain randomness, such as the input of flow, the proportion of off-ramp vehicles, and the length of the MLC zone. In addition, the research object explored in this paper is a freeway. When the vehicle is driving near the off-ramp of an urban road, changes to the above factors should also be considered. In our analysis of the simulation results, it has been mentioned that the operation efficiency of the traffic flow can be improved to a certain extent by extending the length of the mandatory lane change area, but when the adjustment ability of this method is exceeded, traffic management can be considered in terms of combining a traffic prediction algorithm, a variable speed limit, and other means of control.

In addition, with the further development of automatic driving technology, a sensing system equipped with more advanced sensors will make the information interaction between the vehicle and road environment more rapid, and the data sources will be more abundant. The algorithms for car-following and changing lanes will then incorporate more factors. For example, the lane-change decisions of vehicles will involve interaction with surrounding vehicles, coordinated lane changes between connected autonomous vehicles, and the coordinated lane changes of connected autonomous vehicle platoons. These factors will be considered in the future modeling of mixed traffic scenarios addressing the off-ramp diversion area.

Author Contributions: Writing—original draft preparation, X.C.; writing—review and editing, Y.L. and Z.W.; supervision, X.C. All authors have read and agreed to the published version of the manuscript.

Funding: This work is supported by the National Natural Science Foundation of China (Grant No. 52172330 and Grant No. 52002281).

Institutional Review Board Statement: Not applicable.

Informed Consent Statement: Not applicable.

Data Availability Statement: Not applicable.

Conflicts of Interest: The authors declare no conflict of interest.

References

1. Li, T.; Kockelman, K. Valuing the Safety Benefits of Connected and Automated Vehicle Technologies. In Proceedings of the Transportation Research Board 95th Annual Meeting, Washington, DC, USA, 10–14 January 2016.
2. Liu, J.; Khattak, A.J. Delivering improved alerts, warnings, and control assistance using basic safety messages transmitted between connected vehicles. *Transp. Res. Part C Emerg. Technol.* **2016**, *68*, 83–100. [[CrossRef](#)]
3. Letter, C.; Elefteriadou, L. Efficient control of fully automated connected vehicles at freeway merge segments. *Transp. Res. Part C Emerg. Technol.* **2017**, *80*, 190–205. [[CrossRef](#)]
4. Tientrakool, P.; Ho, Y.C.; Maxemchuk, N.F. Highway Capacity Benefits from Using Vehicle-to-Vehicle Communication and Sensors for Collision Avoidance. In Proceedings of the 2011 IEEE Vehicular Technology Conference (VTC Fall), San Francisco, CA, USA, 5–8 September 2011; pp. 1–5.
5. Jiang, H.; Hu, J.; An, S.; Wang, M.; Park, B.B. Eco approaching at an isolated signalized intersection under partially connected and automated vehicles environment. *Transp. Res. Part C Emerg. Technol.* **2017**, *79*, 290–307. [[CrossRef](#)]
6. Yang, H.; Rakha, H.; Ala, M.V. Eco-cooperative adaptive cruise control at signalized intersections considering queue effects. *IEEE Trans. Intell. Transp. Syst.* **2016**, *18*, 1575–1585. [[CrossRef](#)]

7. Wang, Z.; Wu, G.; Barth, M.J. Cooperative Eco-Driving at Signalized Intersections in a Partially Connected and Automated Vehicle Environment. *IEEE Trans. Intell. Transp. Syst.* **2019**, *21*, 2029–2038. [[CrossRef](#)]
8. Talebpour, A.; Mahmassani, H.S. Influence of connected and autonomous vehicles on traffic flow stability and throughput. *Transp. Res. Part C Emerg. Technol.* **2016**, *71*, 143–163. [[CrossRef](#)]
9. Dong, C.Y.; Wang, H.; Wang, W.; Li, Y.; Hua, X.D. Hybrid traffic flow model for intelligent vehicles exiting to off-ramp. *Acta Phys. Sin.* **2018**, *67*, 144501. [[CrossRef](#)]
10. Zhang, Y.; Ioannou, P.A. Combined Variable Speed Limit and Lane Change Control for Highway Traffic. *IEEE Trans. Intell. Transp. Syst.* **2017**, *18*, 1812–1823. [[CrossRef](#)]
11. Xiao, L.; Gao, F. A comprehensive review of the development of adaptive cruise control systems. *Veh. Syst. Dyn.* **2010**, *48*, 1167–1192. [[CrossRef](#)]
12. Shaout, A.; Tarrach, M.A. Cruise control technology review. *Comput. Electr. Eng.* **1997**, *23*, 259–271. [[CrossRef](#)]
13. Jiang, R.; Wu, Q.; Zhu, Z. Full velocity difference model for a car-following theory. *Phys. Rev. E* **2001**, *64*, 017101. [[CrossRef](#)]
14. Treiber, M.; Hennecke, A.; Helbing, D. Congested traffic states in empirical observations and microscopic simulations. *Phys. Rev. E* **2000**, *62*, 1805. [[CrossRef](#)] [[PubMed](#)]
15. Shladover, S.E.; Su, D.; Lu, X.Y. Impacts of Cooperative Adaptive Cruise Control on Freeway Traffic Flow. *Transp. Res. Rec.* **2012**, *2324*, 63–70. [[CrossRef](#)]
16. Milanés, V.; Shladover, S.E.; Spring, J.; Nowakowski, C.; Kawazoe, H.; Nakamura, M. Cooperative Adaptive Cruise Control in Real Traffic Situations. *IEEE Trans. Intell. Transp. Syst.* **2014**, *15*, 296–305. [[CrossRef](#)]
17. Milanés, V.; Shladover, S.E. Modeling cooperative and autonomous adaptive cruise control dynamic responses using experimental data. *Transp. Res. Part C Emerg. Technol.* **2014**, *48*, 285–300. [[CrossRef](#)]
18. Hidas, P. Modelling lane changing and merging in microscopic traffic simulation. *Transp. Res. Part C Emerg. Technol.* **2002**, *10*, 351–371. [[CrossRef](#)]
19. Yang, X.B. A lane changing model considering the maneuver process and its applications. *Acta Phys. Sin.* **2009**, *58*, 836–842. [[CrossRef](#)]
20. Zheng, Z.; Ahn, S.; Chen, D.; Laval, J. The effects of lane changing on the immediate follower: Anticipation, relaxation, and change in driver characteristics. *Transp. Res. Part C Emerg. Technol.* **2013**, *26*, 367–379. [[CrossRef](#)]
21. Nilsson, P.; Laine, L.; Sandin, J.; Jacobson, B.; Eriksson, O. On actions of long combination vehicle drivers prior to lane changes in dense highway traffic a driving simulator study. *Transp. Res. Part F Traffic Psychol. Behav.* **2018**, *55*, 25–37. [[CrossRef](#)]
22. Gazis, D.C.; Herman, R.; Rothery, R.W.; Ni, D.; Leonard, J.D.; Jia, C.; Wang, J.; Mahmassani, H.S.; Sun, D.; Elefteriadou, L.; et al. Nonlinear Follow-the-Leader Models of Traffic Flow. *Oper. Res.* **1961**, *9*, 545–567. [[CrossRef](#)]
23. Newell, G.F. Nonlinear Effects in the Dynamics of Car Following. *Oper. Res.* **1961**, *9*, 209–229. [[CrossRef](#)]
24. Nagel, K.; Schreckenberg, M. A cellular automaton model for freeway traffic. *J. Phys. I* **1992**, *2*, 2221–2229. [[CrossRef](#)]
25. Rajamani, R.; Shladover, S.E. An Experimental Comparative Study of Autonomous and Co-operative Vehicle-follower Control Systems. *Transp. Res. Part C—Emerg. Technol.* **2001**, *9*, 15–31. [[CrossRef](#)]
26. Kerner, B.S. Experimental features of self-organization in traffic flow. *Phys. Rev. Lett.* **1998**, *81*, 3797–3800. [[CrossRef](#)]
27. Ahmed, K.I. *Modeling Drivers' Acceleration and Lane Changing Behavior*; Massachusetts Institute of Technology: Cambridge, MA, USA, 1999.
28. Zhang, L.; Chen, C.; Zhang, J.; Fang, S.; You, J.; Guo, J. Modeling Lane-Changing Behavior in Freeway Off-Ramp Areas from the Shanghai Naturalistic Driving Study. *J. Adv. Transp.* **2018**, *2018*, 8645709. [[CrossRef](#)]
29. Nafi, N.S.; Khan, R.H.; Khan, J.Y.; Gregory, M. A Predictive Road Traffic Management System Based on Vehicular ad-hoc Network. In Proceedings of the Australasian Telecommunication Networks & Applications Conference IEEE, Southbank, Australia, 26–28 November 2014.
30. Zambrano-Martinez, J.L.; Calafate, C.T.; Soler, D.; Lemus-Zúñiga, L.-G.; Cano, J.-C.; Manzoni, P.; Gayraud, T. A Centralized Route-Management Solution for Autonomous Vehicles in Urban Areas. *Electronics* **2019**, *8*, 722. [[CrossRef](#)]
31. Kesting, A.; Treiber, M.; Helbing, D. Enhanced Intelligent driver model to access the impact of driving strategies on traffic capacity. *Philos. Trans. R. Soc. A Math. Phys. Eng. Sci.* **2010**, *368*, 4585–4605. [[CrossRef](#)]
32. Wang, H.; Qin, Y.; Wang, W.; Chen, J. Stability of CACC-manual heterogeneous vehicular flow with partial CACC performance degrading. *Transp. B Transp. Dyn.* **2018**, *7*, 788–813. [[CrossRef](#)]
33. Milanés, V.; Villagrà, J.; Pérez, J.; González, C. Low-Speed Longitudinal Controllers for Mass-Produced Cars: A Comparative Study. *IEEE Trans. Ind. Electron.* **2012**, *59*, 620–628. [[CrossRef](#)]
34. van Beinum, A.; Farah, H.; Wegman, F.; Hoogendoorn, S. Driving behaviour at motorway ramps and weaving segments based on empirical trajectory data. *Transp. Res. Part C Emerg. Technol.* **2018**, *95*, 426–441. [[CrossRef](#)]
35. Berrazouane, M.; Tong, K.; Solmaz, S.; Kiers, M.; Erhart, J. Analysis and Initial Observations on Varying Penetration Rates of Automated Vehicles in Mixed Traffic Flow utilizing SUMO. In Proceedings of the 2019 IEEE International Conference on Connected Vehicles and Expo (ICCVE), Graz, Austria, 4–8 November 2019; pp. 1–7.

Disclaimer/Publisher's Note: The statements, opinions and data contained in all publications are solely those of the individual author(s) and contributor(s) and not of MDPI and/or the editor(s). MDPI and/or the editor(s) disclaim responsibility for any injury to people or property resulting from any ideas, methods, instructions or products referred to in the content.